*Inorg. Chem.* **2009**, *48*, 45−54

# Design, Synthesis, Characterization, and OFET Properties of Amphiphilic Heteroleptic Tris(phthalocyaninato) Europium(III) Complexes. The Effect of Crown Ether Hydrophilic Substituents

**Yingning Gao,[†] Pan Ma,[†] Yanli Chen,[†,‡] Ying Zhang,[†] Yongzhong Bian,[†] Xiyou Li,[†] Jianzhuang Jiang,[*,†] and Changqin Ma[*,†]**

*Department of Chemistry, Shandong University, Jinan 250100, China, and Department of Chemistry, Jinan University, Jinan 250001, China*

Received June 6, 2008

Two amphiphilic heteroleptic tris(phthalocyaninato) europium complexes with hydrophilic crown ether heads and hydrophobic octyloxy tails [Pc(*m*C*n*)$_4$]Eu[Pc(*m*C*n*)$_4$]Eu[Pc(OC$_8$H$_{17}$)$_8$] [*m* = 12, *n* = 4, H$_2$Pc(12C4)$_4$ = 2,3,9,10,16,17,23,24-tetrakis(12-crown-4)phthalocyanine; *m* = 18, *n* = 6, H$_2$Pc(18C6)$_4$ = 2,3,9,10,16,17,23,24-tetrakis(18-crown-6)phthalocyanine; H$_2$Pc(OC$_8$H$_{17}$)$_8$ = 2,3,9,10,16,17,23,24-octakis(octyloxy)phthalocyanine] (**1**, **2**) were designed and prepared from the reaction between homoleptic bis(phthalocyaninato) europium compound [Pc(*m*C*n*)$_4$]Eu[Pc(*m*C*n*)$_4$] (*m* = 12, *n* = 4; *m* = 18, *n* = 6) and metal-free H$_2$Pc(OC$_8$H$_{17}$)$_8$ in the presence of Eu(acac)$_3$·H$_2$O (Hacac = acetylacetone) in boiling 1,2,4-trichlorobenzene. These novel sandwich triple-decker complexes were characterized by a wide range of spectroscopic methods and electrochemically studied. With the help of the Langmuir−Blodgett technique, these typical amphiphilic triple-decker complexes were fabricated into organic field effect transistors (OFET) with top contact configuration on bare SiO$_2$/Si substrate, hexamethyldisilazane-treated SiO$_2$/Si substrate, and octadecyltrichlorosilane (OTS)-treated SiO$_2$/Si substrate, respectively. The device performance is revealed to be dependent on the species of crown ether substituents and substrate surface treatment. OFETs fabricated from the triple decker with 12-crown-4 hydrophilic substituents, **1**, allow the hole transfer in the direction parallel to the aromatic phthalocyanine rings. In contrast, the devices of a triple-decker compound containing 18-crown-6 as hydrophilic heads, **2**, transfer holes in a direction along the long axis of the assembly composed of face-to-face aggregated triple-decker molecules, revealing the effect of molecular structure, specifically the crown ether substituents on the film structure and OFET functional properties. The carrier mobility for hole as high as 0.33 cm$^2$ V$^{-1}$ s$^{-1}$ and current modulation of 7.91 × 10$^5$ were reached for the devices of triple-decker compound **1** deposited on the OTS-treated SiO$_2$/Si substrates, indicating the effect of substrate surface treatment on the OFET performance due to the improvement on the film quality as demonstrated by the atomic force microscope investigation results.

## Introduction

Organic semiconductors have attracted significant research interest since 1987 when they were first constructed into organic field effect transistors (OFETs) as active layers.[1] Great industrial interests for the OFETs come from their potential applications in low-end electronics market because of their advantages over conventional silicon technology such as large area and flexible displayer, active-matrix electronic paper, and simple low-cost memory devices such as smart cards and price tags.[2−11] Although the performance of the

* To whom correspondence should be addressed. E-mail: jzjiang@sdu.edu.cn; cqma@crystech.com.
† Shandong University.
‡ Jinan University.

(1) Koezuka, H.; Tsumura, A.; Ando, T. *Synth. Met.* **1987**, *18*, 699–704.
(2) Horowitz, G. *Adv. Mater.* **1998**, *10*, 365–377.
(3) Fichou, D. *J. Mater. Chem.* **2000**, *10*, 571–588.
(4) Katz, H. E.; Bao, Z. *J. Phys. Chem. B* **2000**, *104*, 671–678.
(5) Katz, H. E.; Bao, Z.; Gilat, S. L. *Acc. Chem. Res.* **2001**, *34*, 359–369.
(6) Würthner, F. *Angew. Chem., Int. Ed.* **2001**, *40*, 1037–1039.
(7) Dimitrakopoulos, C. D.; Malenfant, P. R. L. *Adv. Mater.* **2002**, *14*, 99–117.
(8) Veres, J.; Ogier, S.; Lloyd, G.; de Leeuw, D. *Chem. Mater.* **2004**, *16*, 4543–4555.
(9) Sun, Y.; Liu, Y.; Zhu, D. *J. Mater. Chem.* **2005**, *15*, 53–65.
(10) Sirringhaus, H. *Adv. Mater.* **2005**, *17*, 2411–2425.
(11) Bao, Z. *Adv. Mater.* **2000**, *12*, 227–230.

10.1021/ic801040z CCC: $40.75 
Published on Web 11/26/2008

**Scheme 1.** Schematic Molecular Structures of Phthalocyanine Ligands and Amphiphilic Heteroleptic Tris(phthalocyaninato) Rare Earth Triple-Decker Complexes $[Pc(12C4)_4]Eu[Pc(12C4)_4]Eu[Pc(OC_8H_{17})_8]$ (**1**) and $[Pc(18C6)_4]Eu[Pc(18C6)_4]Eu[Pc(OC_8H_{17})_8]$ (**2**)

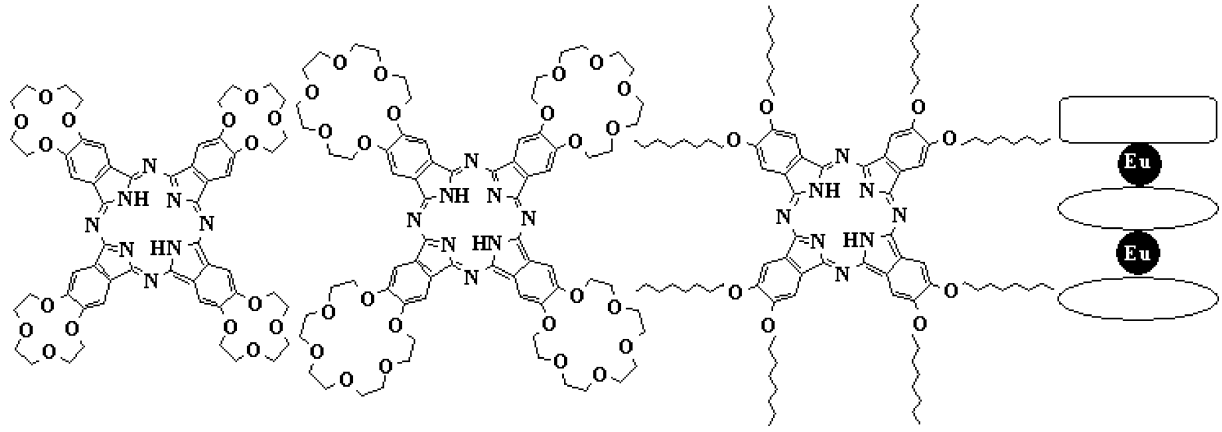


organic materials-based field effect transistor (FET) achieved thus far still cannot compete with the widely utilized inorganic analogues (i.e., the amorphous hydrogenated silicon (a-Si:H) FETs with field effect mobility $\mu = 1$ cm$^2$ V$^{-1}$ s$^{-1}$ and current modulation of $10^6$), significant progress has been made in the past decade toward understanding OFETs and realizing their industrial applications.

Phthalocyanines have been an important industrial commodity used as inks and dyestuffs since their first synthesis early in the last century.[12] Associated with their large conjugated molecular structure, these macromolecules have been among the most intensively studied organic semiconductors for OFETs because of their high thermal and chemical stability.[13] Recently, inspired by the early pioneering work of Simon and co-workers in the semiconductivity of unsubstituted bis(phthalocyaninato) rare earth complexes $M(Pc)_2$ (M = Tm, Lu),[14] the OFET properties of substituted phthalocyanine-containing sandwich complexes of rare earth such as heteroleptic bis(phthalocyaninato) rare earth double-deckers $M(Pc)[Pc(OC_8H_{17})_8]$ (M = Tb, Lu) started to attract research interest because of their potential solution processing ability associated with their increased solubility in common organic solvents.[15] In particular, the solution-processed OFETs fabricated from amphiphilic tris(phthalocyaninato) rare earth triple-decker complexes $[Pc(15C5)_4]M[Pc(15C5)_4]M[Pc(OC_8H_{17})_8]$ (M = Eu, Tb, Lu) have been revealed to display excellent FET performance with the carrier mobility as high as 0.60 cm$^2$ V$^{-1}$ s$^{-1}$ and current modulation of $10^5$.[16] This led to the synthesis, characterization, and systematic investigation for the semiconductor properties of a series amphiphilic tris(phthalocyaninato) rare earth triple-decker complexes including $[Pc(15C5)_4]Eu[Pc(15C5)_4]Eu[Pc(OC_nH_{2n+1})_8]$($n$=4,6,8,10,12)[17] and $\{Pc[(OC_2H_4)_2OCH_3]_8\}Eu\{Pc[(OC_2H_4)_2OCH_3]_8\}Eu[Pc(OC_nH_{2n+1})_8]$ ($n$ = 6, 8, 10, 12).[18] For the purpose of knowing the effect of molecular structure on the OFET functional properties, it appears necessary to design, prepare, and investigate the OFET performance of corresponding sandwich triple-decker complexes of rare earth containing phthalocyanine ligands with hydrophilic 12-crown-4 and 18-crown-6 moieties.

In the present article, we describe the synthesis, spectroscopic, and electrochemical properties of two novel amphiphilic tris(phthalocyaninato) europium(III) complexes with hydrophilic 12-crown-4 or 18-crown-6 heads and hydrophobic octyloxy tails $[Pc(mCn)_4]Eu[Pc(mCn)_4]Eu[Pc(OC_8H_{17})_8]$ ($m$ = 12, $n$ = 4; $m$ = 18, $n$ = 6) (**1**, **2**) (Scheme 1). In particular, these typical amphiphilic sandwich triple-decker molecules have been fabricated into OFET devices by the Langmuir−Blodgett (LB) technique after surface treatment for the $SiO_2$/Si substrates, which show good OFET performance with carrier mobility as high as 0.33 cm$^2$ V$^{-1}$ s$^{-1}$ and current modulation of $7.91 \times 10^5$ in the direction parallel to the aromatic phthalocyanine rings for compound **1** and in a direction along the long axis of the assembly composed of face-to-face aggregated triple-decker molecules for **2**. The present work not only develops a new series of sandwich phthalocyaninato rare earth complexes as novel organic semiconductors but also more importantly represents the new effort toward better understanding of the relationship between

(12) (a) *Phthalocyanines: Properties and Applications*; Lever, A. B. P., Leznoff, C. C., Eds.; VCH: New York, 1989; Vols. *1*−*4*. (b) McKeown, N. B. *Phthalocyanine Materials: Synthesis, Structure, and Function*; Cambridge University Press: New York, 1998. (c) *The Porphyrin Handbook*; Kadish, K. M., Smith, K. M., Guilard, R., Eds.; Academic Press: San Diego, CA, 2000, 2003; Vols. *1*−*20*.

(13) (a) Bao, Z.; Lovinger, A. J.; Dodabalapur, A. *Appl. Phys. Lett.* **1996**, *69*, 3066–3068. (b) Bao, Z.; Lovinger, A. J.; Brown, J. *J. Am. Chem. Soc.* **1998**, *120*, 207–208. (c) Mizuno, E.; Taniguchi, M.; Kawai, T. *Appl. Phys. Lett.* **2005**, *86*, 143513–143515. (d) Ofuji, M.; Ishikawa, K.; Takezoe, H. *Appl. Phys. Lett.* **2005**, *86*, 062114–062116. (e) Lochlin, J.; Shinbo, K.; Onishi, K.; Kaneko, F.; Bao, Z.; Advincula, R. C. *Chem. Mater.* **2003**, *15*, 1404–1412. (f) Zhang, J.; Wang, J.; Wang, H.; Yan, D. *Appl. Phys. Lett.* **2004**, *84*, 142–144. (g) Xiao, K.; Liu, Y.; Huang, X.; Xu, Y.; Yu, G.; Zhu, D. *J. Phys. Chem. B* **2003**, *107*, 9226–9230. (h) Bora, M.; Schut, D.; Baldo, M. A. *Anal. Chem.* **2007**, *79*, 3298–3303. (i) Tang, Q.; Li, H.; Liu, Y.; Hu, W. *J. Am. Chem. Soc.* **2006**, *128*, 14634–14639.

(14) (a) Simon, J.; Andre, J. *Molecular Semiconductors*; Springer-Verlag: Berlin, 1985. (b) Bouvet, M.; Simon, J. *Chem. Phys. Lett.* **1990**, *172*, 299–302.

(15) (a) Jiang, J.; Ng, D. K. P. *Acc. Chem. Res.* [Online early access]. DOI: 10.1021/ar800097s. Published Online: Nov 13, 2008. http://pubs.acs.org/doi/abs/10.1021/ar800097s. (b) Su, W.; Jiang, J.; Xiao, K.; Chen, Y.; Zhao, Q.; Yu, G.; Liu, Y. *Langmuir* **2005**, *21*, 6527–6531.

(16) Chen, Y.; Su, W.; Bai, M.; Jiang, J.; Li, X.; Liu, Y.; Wang, L.; Wang, S. *J. Am. Chem. Soc.* **2005**, *127*, 15700–15701.

(17) Chen, Y.; Li, R.; Wang, R.; Ma, P.; Dong, S.; Gao, Y.; Li, X.; Jiang, J. *Langmuir* **2007**, *23*, 12549–12554.

(18) Li, R.; Ma, P.; Dong, S.; Zhang, X.; Chen, Y.; Li, X.; Jiang, J. *Inorg. Chem.* **2007**, *46*, 11397–11404.

**Scheme 2.** Synthesis of 4,5-Di(12-crown-4)phthalonitrile and Homoleptic Bis[2,3,9,10,16,17,23,24-tetrakis(12-crown-4)phthalocyaninato] Europium Complex

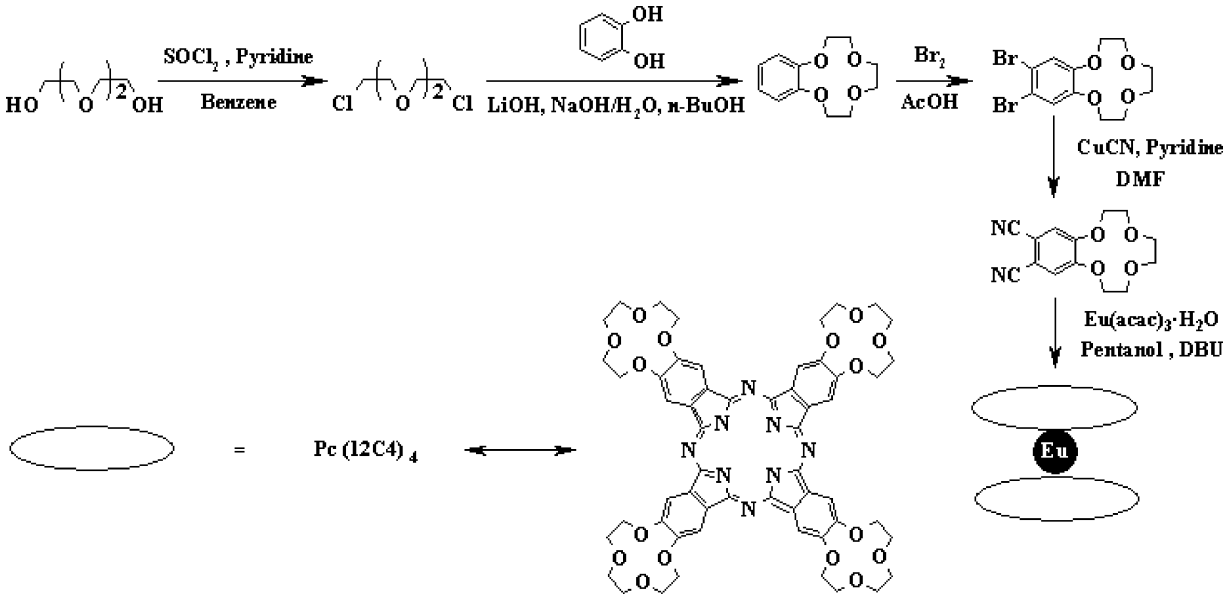


the molecular structure, film structure, and OFET functional properties.

## Results and Discussion

**Synthesis.** It is noteworthy that crown ether-substituted phthalocyanine-containing sandwich rare earth complexes, in particular M(Pc)[Pc(15C5)$_n$] (M = Eu, Lu; $n$ = 1−4), have been intensively studied as the bridge to link the gap between the electronic structures of bis(phthalocyaninato) rare earth double deckers and infinite supramolecular phthalocyanine one-dimensional stacks or polymers.[19] However, crown ethers other than 15-crown-5-substituted phthalocyanine-containing rare earth complexes with sandwich structure have not yet been reported. Actually, to the best of our knowledge, there is even no report on the 12-crown-4-substituted phthalocyanine thus far. As a result, in the present case, the precursor of 2,3,9,10,16,17,23,24-tetrakis(12-crown-4)phthalocyanine, 4,5-dicyanobenzo-12-crown-4, has to be designed and prepared first. When a similar pathway was used to prepare 4,5-dicyanobenzo-15-crown-5[20] (Scheme 2) with triethyleneglycol as starting material after a series of reactions involving chlorination, etherification, bromination, and cyanation, 4,5-dicyanobenzo-12-crown-4 was synthesized for the first time.

4,5-Dicyanobenzo-18-crown-6, the precursor of 2,3,9,10,16,17,23,24-tetrakis(18-crown-6)phthalocyanine, was prepared using commercially available benzo-18-crown-6 according to the published procedure.[21] Despite the well-described spectroscopic characterization, the molecular structure of this compound has not yet been resolved by X-ray diffraction analysis. Single crystal of 4,5-di(18-crown-6)phthalonitrile suitable for X-ray analysis was obtained by diffusion of ethanol into the chloroform solution of this compound. Figure 1 shows the molecular structure of 4,5-di(18-crown-6)phthalonitrile in top view. As shown in this figure, two cyano groups are coplanar with the benzene ring and the two C−N bond lengths are almost equal, with an average value of 1.12 Å. The section of 18-crown-6 in this compound has a crown-like shape that is typical for $D_{3d}$ conformation, and the mean deviation of six oxygen atoms from their least-squares plane is within ±0.32 Å.

As expected, cyclic tetramerization of 4,5-dicyanobenzo-12-crown-4 or 4,5-dicyanobenzo-18-crown-6 in the presence of Eu(acac)$_3$·H$_2$O promoted with organic base 1,8-diazabicyclo[5.4.0]undec-7-ene provides the homoleptic tetrakis(*m*-crown-*n*)-substituted bis(phthalocyaninato) europium compounds [Pc(*m*C*n*)$_4$]Eu[Pc(*m*C*n*)$_4$] ($m$ = 12, $n$ = 4; $m$ =

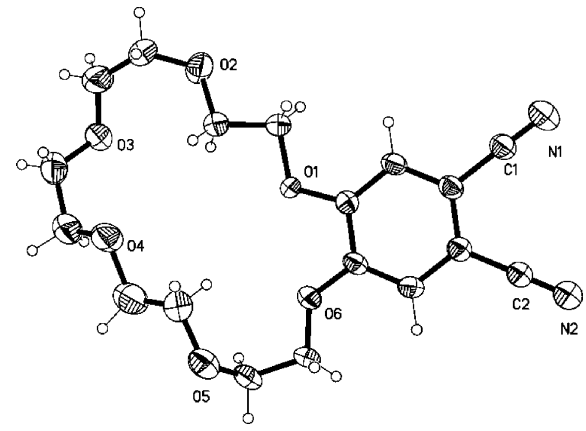


**Figure 1.** Molecular structure of 4,5-di(18-crown-6)phthalonitrile in top view showing the 30% probability thermal ellipsoids for all atoms.

(19) (a) Sheng, N.; Li, R.; Choi, C.-F.; Su, W.; Ng, D. K. P.; Cui, X.; Yoshida, K.; Kobayashi, N.; Jiang, J. *Inorg. Chem.* **2006**, *45*, 3794–3802. (b) Ishikawa, N.; Kaizu, Y. *Chem. Phys. Lett.* **1993**, *203*, 472–476. (c) Ishikawa, N.; Kaizu, Y. *Mol. Cryst. Liq. Cryst.* **1996**, *286*, 263–268. (d) Ishikawa, N.; Kaizu, Y. *Chem. Lett.* **1998**, *27*, 183–184. (e) Ishikawa, N.; Kaizu, Y. *J. Phys. Chem. A* **2000**, *104*, 10009–10016. (f) Ishikawa, N.; Kaizu, Y. *Coord. Chem. Rev.* **2002**, *226*, 93–101.

(20) Sielcken, O. E.; Van Tilborg, M. M.; Roks, M. F. M.; Hendriks, R.; Drenth, W.; Nolte, R. J. M. *J. Am. Chem. Soc.* **1987**, *109*, 4261–4265.

18, $n = 6$),[22] which represent the first example of sandwich bis(phthalocyaninato) europium complexes with either 12-crown-4 or 18-crown-6 moieties. Metal-free phthalocyanine with eight octyloxy groups at the peripheral positions $H_2Pc(OC_8H_{17})_8$ was prepared following the standard method.[23] When a similar methodology was used to prepare 15-crown-5-substituted phthalocyanine-containing analogues $[Pc(15C5)_4]M[Pc(15C5)_4]M[Pc(OC_nH_{2n+1})_8]$ (M = Eu, Tb, Lu; $n = 4, 6, 8, 10, 12$),[16,17] condensation of monomeric $[Pc(OC_8H_{17})_8]Eu(acac)$, generated in situ from $Eu(acac)_3 \cdot H_2O$ and $H_2Pc(OC_8H_{17})_8$, and $[Pc(mCn)_4]Eu[Pc(mCn)_4]$ in refluxing 1,2,4-trichlorobenzene (TCB) led to the isolation of typical amphiphilic heteroleptic tris(phthalocyaninato) europium complexes $[Pc(mCn)_4]Eu[Pc(mCn)_4]Eu[Pc(OC_8H_{17})_8]$ ($m = 12$, $n = 4$; $m = 18$, $n = 6$) (**1**, **2**) in relatively good yield, which, however, is lower than that for 15-crown-5-substituted phthalocyanine-containing analogue $[Pc(15C5)_4]Eu[Pc(15C5)_4]Eu[Pc(OC_8H_{17})_8]$.[16]

Satisfactory elemental analysis results were obtained for both of the newly prepared heteroleptic amphiphilic europium triple-decker complexes **1** and **2**, which have good solubility in common organic solvents such as $CHCl_3$, $CH_2Cl_2$, and toluene, after repeated column chromatography and recrystallization. They were also characterized by MALDI-TOF mass and $^1H$ NMR spectroscopies. The MALDI-TOF mass spectra of these compounds clearly showed intense signals for the molecular ion $(M)^+$. The isotopic pattern closely resembles the simulated one as exemplified by the spectrum of compound **1** given in Figure S1 in the Supporting Information.

**Spectroscopic Characteristics.** The electronic absorption spectra of triple-decker complexes (**1**, **2**) together with double-deckers $Eu[Pc(mCn)_4]_2$ ($m = 12$, $n = 4$; $m = 18$, $n = 6$) were recorded in chloroform, and the data are summarized in Table S1 in the Supporting Information. Figure 2 displays the electronic absorption spectra of the heteroleptic triple-decker complexes in comparison with those in the LB film. The solution spectra are analogous to those reported for related tris(phthalocyaninato) rare earth

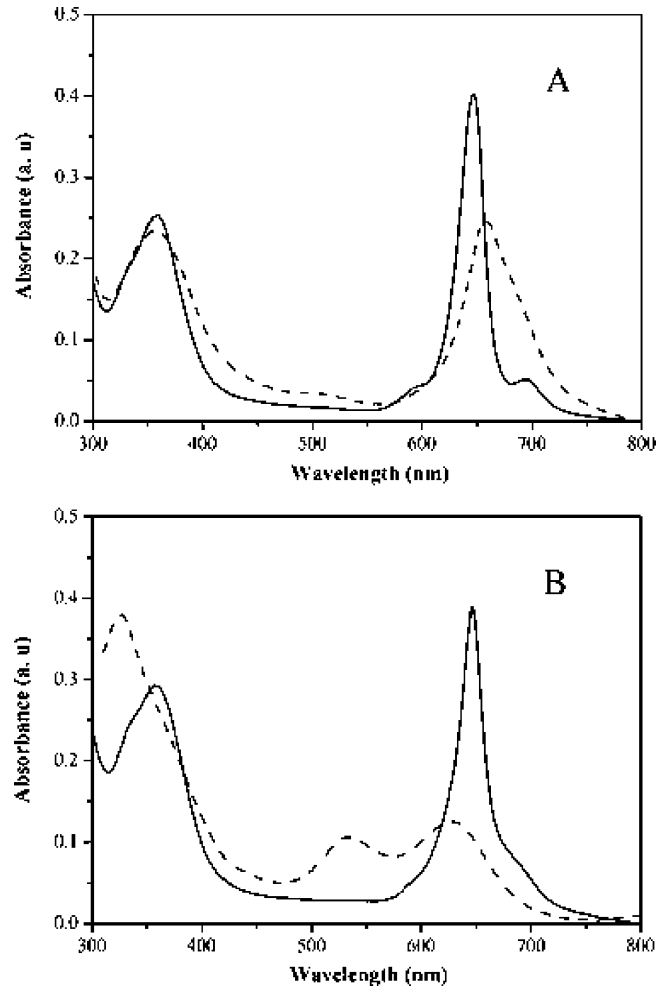


**Figure 2.** Electronic absorption spectra of compounds **1** (A) and **2** (B) in solution (solid line) and in LB film (dash line).

compounds[24,25] and in particular $[Pc(15C5)_4]M[Pc(15C5)_4]M[Pc(OC_nH_{2n+1})_8]$ (M = Eu, Tb, Lu; $n = 4, 6, 8, 10, 12$).[16,17] The absorption around 358 nm in chloroform can be attributed to the phthalocyanine Soret band for both **1** and **2**, while the strong band around 647 nm and a weak satellite absorption around 694 nm are the phthalocyanine Q bands.

The $^1H$ NMR spectra of both the newly prepared triple-decker compounds **1** and **2** were recorded in $CDCl_3$ at room temperature. Figure S2 in the Supporting Information exhibits the $^1H$ NMR spectrum of compound **1** in $CDCl_3$. Three singlet signals appearing in the low field region at $\delta$ 12.52, 9.67, and 9.29 are obviously due to the $\alpha$ protons of the three Pc rings, respectively, of the triple-decker compound **1**. The aliphatic proton signals from the octyloxy side chains of $Pc(OC_8H_{17})_8$ are observed in the high field range, some of which are located in the same area as those of the 12-crown-4 ether substituents. However, with the help of the $^1H$-$^1H$ COSY spectrum, as shown in Figure S3 in the Supporting Information, clear assignments to different protons in either octyloxy or 12-crown-4 ether substituents can be easily reached.

(21) Pedersen, C. J. *J. Am. Chem. Soc.* **1967**, *89*, 7017–7036.
(22) (a) Bai, M.; Bao, M.; Ma, C.; Arnold, D. P.; Choi, M. T. M.; Ng, D. K. P.; Jiang, J. *J. Mater. Chem.* **2003**, *13*, 1333–1339. (b) Yoshimoto, S.; Sawaguchi, T.; Su, W.; Jiang, J. *J. Mater. Chem.* **2003**, *13*, 1333–1339. (c) Zhu, P.; Pan, N.; Li, R.; Dou, J.; Zhang, Y.; Cheng, D. Y. Y.; Wang, D.; Ng, D. K. P.; Jiang, J. *Chem.−Eur. J.* **2005**, *11*, 1425–1432. (d) Takami, T.; Arnold, D. P.; Fuchs, A. V.; Will, G. D.; Goh, R.; Waclawik, E. R.; Bell, J. M.; Weiss, P. S.; Sugiura, K.-I.; Liu, W.; Jiang, J. *J. Phys. Chem. B* **2006**, *110*, 1661–1664. (e) Chen, Y.; Liu, H.-G.; Zhu, P.; Zhang, Y.; Wang, X.; Li, X.; Jiang, J. *Langmuir* **2005**, *21*, 11289–11295.
(23) Li, R.; Zhang, X.; Zhu, P.; Li, X.; Ng, D. K. P.; Kobayashi, N.; Jiang, J. *Inorg. Chem.* **2006**, *45*, 2327–2334.
(24) (a) Liu, W.; Jiang, J.; Arnold, D. P.; Pan, N. *Inorg. Chim. Acta* **2000**, *310*, 140–146. (b) Arnold, D. P.; Jiang, J. *J. Phys. Chem. A* **2001**, *105*, 7525–7533. (c) Zhu, P.; Pan, N.; Li, R.; Dou, J.; Zhang, Y.; Cheng, D. Y. Y.; Wang, D.; Ng, D. K. P.; Jiang, J. *Chem.−Eur. J.* **2005**, *11*, 1425–1432. (d) Bian, Y.; Li, L.; Wang, D.; Choi, C.-F.; Cheng, D. Y. Y.; Zhu, P.; Li, R.; Dou, J.; Wang, R.; Pan, N.; Ng, D. K. P.; Kobayashi, N.; Jiang, J. *Eur. J. Inorg. Chem.* **2005**, 2612–2618.
(25) (a) Ishikawa, N.; Iino, T.; Kaizu, Y. *J. Am. Chem. Soc.* **2002**, *124*, 11440–11447. (b) Ishikawa, N.; Iino, T.; Kaizu, Y. *J. Phys. Chem. A* **2002**, *106*, 9543–9550. (c) Ishikawa, N.; Iino, T.; Kaizu, Y. *J. Phys. Chem. A* **2003**, *107*, 7879–884. (d) Ishikawa, N.; Otsuka, S.; Kaizu, Y. *Angew. Chem., Int. Ed.* **2005**, *44*, 731–733.

**Table 1.** Half-Wave Redox Potentials of Triple-Deckers **1**, **2**, and $[Pc(15C5)_4]Eu[Pc(15C5)_4]Eu[Pc(OC_8H_{17})_8]$ in $CH_2Cl_2$ Containing 0.1 M TBAP

| compd | $Oxd_4$ | $Oxd_3$ | $Oxd_2$ | $Oxd_1$ | $Red_1$ | $Red_2$ | $\Delta E^o_{1/2}$[a] |
|---|---|---|---|---|---|---|---|
| **1** | +1.38 | +0.95 | +0.54 | +0.26 | −0.70 | −1.09 | 0.96 |
| $Eu_2[Pc(15C5)_4]_2[Pc(OC_8H_{17})_8]$ | +1.41 | +1.04 | +0.47 | +0.23 | −0.79 | −1.13 | 1.02 |
| **2** | +1.29 | +1.06 | +0.54 | +0.20 | −0.82 | −1.20 | 1.02 |

[a] $\Delta E^o_{1/2}$ is the potential difference between the first oxidation and first reduction processes (i.e., the HOMO−LUMO gap of corresponding molecule).

For these two heteroleptic tris(phthalocyaninato) europium compounds **1** and **2**, the characteristic phthalocyanine dianion IR bands for both $[Pc(12C4)_4]^{2-}$/$[Pc(18C6)_4]^{2-}$ and $[Pc(OC_8H_{17})_8]^{2-}$ at ca. 1384 $cm^{-1}$ attributed to the symmetric C−H bendings of $-CH_3$ groups in side chains of phthalocyanine rings together with the isoindole stretching vibrations are observed in these spectra.[26] The intense absorption bands observed, respectively, at ca. 1089 and 1277 $cm^{-1}$ are attributed to the symmetric and asymmetric C−O−C stretching. The intense absorption bands at ca. 2856 (symmetric), 2873 (antisymmetric), and 2926 $cm^{-1}$ (symmetric) in the IR spectra are attributed to the C−H stretching vibrations of the $-CH_2-$ and $-CH_3$ groups of the side chains, respectively.

**Electrochemical Properties.** The electrochemical behavior of both triple-decker complexes was investigated by cyclic voltammetry (CV) and differential pulse voltammetry (DPV) in $CH_2Cl_2$. These triple-decker compounds display four one-electron oxidations labeled as $Oxd_1$−$Oxd_4$ and two one-electron reductions ($Red_1$−$Red_2$) within the electrochemical window of $CH_2Cl_2$ under the present conditions. The separation between the reduction and oxidation peak potentials for each process is 65−90 mV. All these processes are attributed to successive removal from, or addition of one electron to, the ligand-based orbitals since the oxidation state of the central tervalent europium ions in triple-decker complexes does not change. The half-wave redox potential values vs SCE are summarized in Table 1. In line with the result on the analogous $[Pc(15C5)_4]Eu[Pc(15C5)_4]Eu[Pc(OC_8H_{17})_8]$, the difference of the redox potential between the first oxidation and first reduction for **1** and **2** is 0.96 and 1.02 V, respectively.

**Film Characterization and OFET Properties.** Reproducible pressure−surface area ($\pi$−$A$) isotherms for **1** and **2** indicate that both compounds can form a stable monolayer on pure water surface because of their typical amphiphilic properties (Figure 3). The limiting molecular area obtained by extrapolation of the liquid−condensed phase to surface pressure zero is 6.94 and 3.60 $nm^2$, respectively, for **1** and **2**. The former value is close to the area of a phthalocyanine ring substituted with four 12-crown-4 moieties, 6.45 $nm^2$, calculated according to the Pcmodel program (Table 2).[27] This suggests that triple-decker molecules of $[Pc(12C4)_4]Eu[Pc(12C4)_4]Eu[Pc(OC_8H_{17})_8]$ (**1**) are lying with a "face-on" orientation on to the water surface. This result is in good agreement with that of analogues $[Pc(15C5)_4]Eu[Pc(15C5)_4]Eu[Pc(OC_nH_{2n+1})_8]$ ($n$ = 4, 6 8, 10, 12)[17] as well as $\{Pc[(OC_2H_4)_2OCH_3]_8\}Eu\{Pc[(OC_2H_4)_2OCH_3]_8\}Eu[Pc(OC_nH_{2n+1})_8]$ ($n$ = 6, 8, 10, 12).[18] The monolayers of $[Pc(12C4)_4]Eu[Pc(12C4)_4]Eu[Pc(OC_8H_{17})_8]$ (**1**) were transferred to hydrophobic substrates by the vertical dipping method, and Z-type LB films were revealed to form for this compound.[28] The fact that the transfer ratio was maintained at an ideal value, 1, during the whole transfer process clearly indicates the formation of uniform thin films with very good layered structure, as shown in Figure S4 in the Supporting Information. However, for $[Pc(18C6)_4]Eu[Pc(18C6)_4]Eu[Pc(OC_8H_{17})_8]$ (**2**), each molecule was revealed to take an area of only 3.60 $nm^2$ on the water surface. The projection of the molecules of compound **2** on the water surface with a "face-on" configuration will show an area of 7.26 $nm^2$, while that of a *face-to-face* orientation and *edge-on* to the water surface gives an area of 3.77 $nm^2$ on the assumption that all the alkoxyl chains extending upward ("face-on" configuration) or bending back ("edge-on" configuration) do not contribute to the molecular area.[17,29] The fact that the limiting area per molecule obtained from the isotherm, 3.60 $nm^2$, is close to the projection of *edge-on* arranged molecule but much

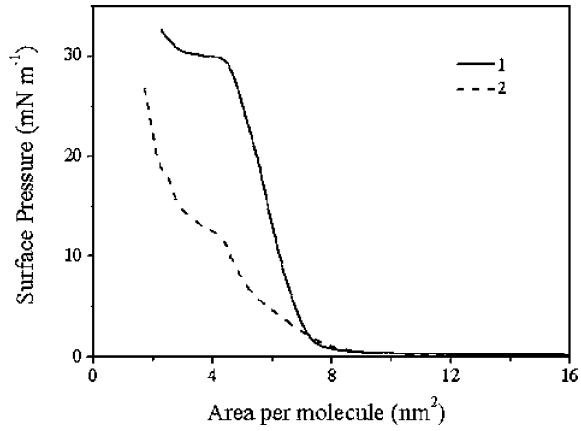


**Figure 3.** $\pi$−$A$ isotherms of compounds **1** and **2** on water surface at room temperature.

**Table 2.** Film Characterization Data and OFET Characteristics of Compounds **1** and **2**

| | compd | **1** | **2** |
|---|---|---|---|
| $\lambda_{max}$ (nm) | $A_{limit}$ ($nm^2$) | 6.94 | 3.60 |
| | solution | 358,647 | 357,646 |
| | LB films | 360,658 | 327,629 |
| | $\Delta\lambda_{max}$ (red shift) | 11 (red shift) | 17 (blue shift) |
| | α (deg)[a] | 21 | 62 |
| | $d$ spacing (nm)[b] | | 2.40 |
| | mobility ($cm^2$ $V^{-1}$ $s^{-1}$) | 0.31 | 0.28 |
| | on/off ratio | $8.59 \times 10^4$ | $1.73 \times 10^5$ |

[a] The dihedral angle between phthalocyanine ring and the surface of substrate determined by polarized UV−vis spectroscopy. [b] Layer spacing determined by low-angle X-ray diffraction experiment.

(26) Jiang, J.; Bao, M.; Rintoul, L.; Arnold, D. P. *Coord. Chem. Rev.* **2006**, *250*, 424–448, and references therein.
(27) *Pcmodel*, version 6.0; Serena Software: Bloomington, IN.
(28) (a) Chen, Y.; Zhang, Y.; Zhu, P.; Fan, Y.; Bian, Y.; Li, X.; Jiang, J. *J. Colloid Interface Sci.* **2006**, *303*, 256–263. (b) Wang, X.; Chen, Y.; Liu, H.; Jiang, J. *Thin Solid Films* **2006**, *496*, 619–625. (c) Chen, Y.; Liu, H.; Zhu, P.; Zhang, Y.; Wang, X.; Li, X.; Jiang, J. *Langmuir* **2005**, *21*, 11289–11295. (d) Chen, Y.; Liu, H.; Pan, N.; Jiang, J. *Thin Solid Films* **2004**, *460*, 279–285.
(29) van Nostrum, C. F.; Picken, S. J.; Schouten, A.-J.; Nolte, R. J. M. *J. Am. Chem. Soc.* **1995**, *117*, 9957–9965.

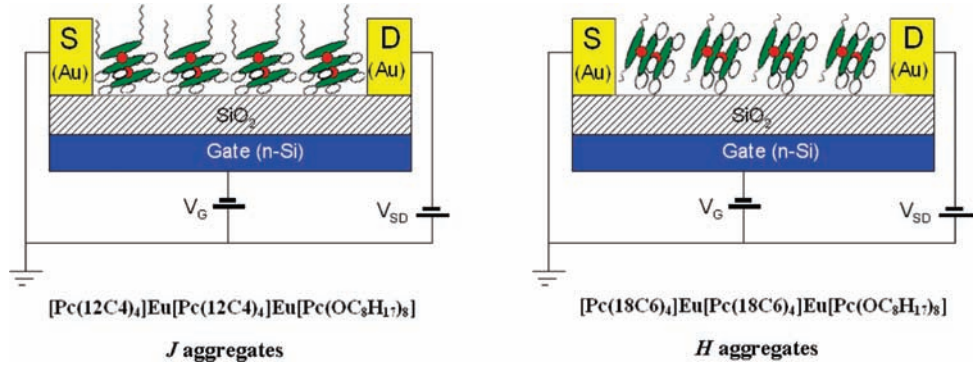


**Figure 4.** Schematic arrangement of heteroleptic tris(phthalocyaninato) europium molecules in the LB film-based OFET devices.

smaller than that of the *face-on* arranged molecule, suggests the triple-decker molecules of compound **2** employ a *face-to-face* stacking with the molecules titled and assembled with the main molecular symmetry axis parallel to the water subphase. It is noteworthy that a similar cofacial configuration was revealed for both metal-free and copper complex of 2,3,9,10,16,17,23,24-octakis[(2-benzyloxy)ethoxy]phthalocyanine on water surface.[30]

The monolayers of $[Pc(18C6)_4]Eu[Pc(18C6)_4]Eu[Pc(OC_8H_{17})_8]$ (**2**) were also transferred to hydrophobic substrates by the vertical dipping method. The transfer ratio was also maintained at an ideal value, 1, during the whole transfer process (Figure S4 in the Supporting Information). Spectroscopic characterization of the two triple-decker compounds **1** and **2** (Figure 2) shows essentially the same absorption in solution. In the LB films, the Q-band of compound **1** makes a red-shift to 658 nm compared with that in solution, 647 nm, as shown in Table S1 in the Supporting Information, indicating the formation of edge-to-edge *J*-aggregates[31] and effective interaction between the neighboring triple-decker molecules in each layer. However, in comparison with the absorption spectrum of compound **2** in solution, a significantly broadened and blue-shifted visible absorption band is observed for the LB film of compound **2**, revealing the formation of face-to-face *H*-aggregates as predicted by the molecular exciton model for dyes in close proximity.[32] In addition, the new absorption band emerging around 535 nm is also a typical sign of the effective $\pi-\pi$ interaction in cofacial configuration of conjugated molecular stacking.[33] This result is in line with that deduced from the $\pi-A$ isotherm studies as detailed above. Considering the same molecular backbone of the two compounds, the change from *J*-aggregates for compound **1** to *H*-aggregates for **2** formed in the LB film, as shown in Figure 4, indicates significant effect of the molecular structure, specifically the crown ether moieties on the molecular packing manner in the films.

Polarized absorption spectroscopic study results reveal that the orientation angle (dihedral angle between phthalocyanine rings and the surface of substrate) of the phthalocyanine ring in these films is ca. 21 and 62° for **1** and **2**, respectively (Table 2).[34] As a consequence, *J*-aggregates should be formed in the LB films of compound **1**, while *H*-aggregates should be formed for compound **2** according to the exciton theory.[35] This result obviously coincides well with that of electronic absorption spectroscopy as discussed above. In addition, the calculated monolayer thickness based on the orientation angle, the octyloxy length of the side groups, and the dimension of the molecule for triple-decker **2**, 2.55 nm, appears to correspond well with the layer spacing (*d*) that resulted from the low-angle X-ray diffraction experiment, 2.40 nm, as shown in Table 2.

The low-angle X-ray diffraction experiment result of LB films for compound **2** shows one diffraction peak corresponding to the *d* spacing of one layer as 2.40 nm (Figure S5 in the Supporting Information). In contrast, no diffraction peak was obtained from low-angle X-ray diffraction experiment for the LB films of compound **1,** implying a molecular packing distorted from the longitudinal direction in multilayer films.[33]

The LB films were also characterized by the atomic force microscope (AFM) technique. Figure 5 compares the phase images of the 10-layer LB films of the compound $[Pc(12C4)_4]Eu[Pc(12C4)_4]Eu[Pc(OC_8H_{17})_8]$ (**1**) on bare $SiO_2$/Si substrate, hexamethyldisilazane (HMDS)-treated $SiO_2$/Si substrate, and octadecyltrichlorosilane (OTS)-treated $SiO_2$/Si substrate, respectively. As can be seen from this figure, on all the substrates, the topographic image shows particular molecular aggregates with spherical domain morphology, consistent with previous experimental result on amphiphilic heteroleptic tris(phthalocyaninato) rare earth analogues

(30) Smolenyak, P. E.; Osburn, J.; Chen, S.-Y.; Chau, L.-K.; O'Brien, D. F.; Armstrong, N. R. *Langmuir* **1997**, *13*, 6568–6576.
(31) Cook, M. J.; Chambrier, I. In *The Porphyrin Handbook*; Kadish, K. M., Smith, K. M., Guilard, R., Eds.; Academic Press: San Diego, CA, 2003; pp 37−127, Vol. *17*.
(32) (a) Kasha, M. In *The Spectroscopy of the Excited State*; Di BartoloB., Ed.; NATO Advanced Study Institute Series B, Physics 12; Plenum Press: New York, 1976; p 337. (b) Kasha, M.; Rawls, H. R.; El-Bayoumi, M. A. *Pure Appl. Chem.* **1965**, *11*, 371–392. (c) Hochstrasser, R. M.; Kasha, M. *Photochem. Photobiol.* **1964**, *3*, 317–331. (d) Chau, L.-K.; England, C. D.; Chen, S.; Armstrong, N. R. *J. Phys. Chem.* **1993**, *97*, 2699–2706.
(33) (a) Würthner, F. *Chem. Commun.* **2004**, *14*, 1564–1579. (b) Balakrishnan, K.; Datar, A.; Naddo, T.; Huang, J.; Oitker, R.; Yen, M.; Zhao, J.; Zang, L. *J. Am. Chem. Soc.* **2006**, *128*, 7390–7398. (c) Kazmaier, P. M.; Hoffmann, R. *J. Am. Chem. Soc.* **1994**, *116*, 9684–9691. (d) Balakrishnan, K.; Datar, A.; Oitker, R.; Chen, H.; Zuo, J.; Zang, L. *J. Am. Chem. Soc.* **2005**, *127*, 10496–10497.
(34) (a) Yoneyama, M.; Sugi, M.; Saito, M.; Ikegama, K.; Kuroda, S.; Iizima, S. *Jpn. J. Appl. Phys.* **1986**, *25*, 961–965. (b) Kobayashi, N.; Lam, H.; Nevin, W. A.; Janda, P.; Leznoff, C. C.; Koyama, T.; Monden, A.; Shiral, H. *J. Am. Chem. Soc.* **1994**, *116*, 879–890.
(35) Kasha, M.; Rawls, H. R.; El-Bayoumi, M. A. *Pure. Appl. Chem.* **1965**, *11*, 371–392.

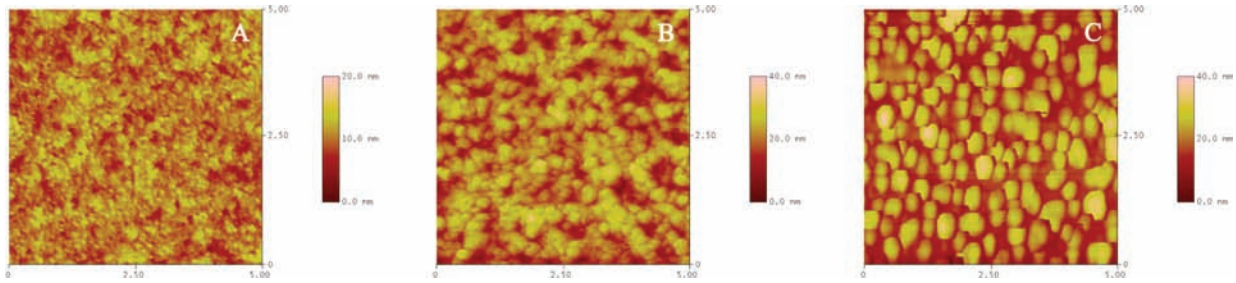


**Figure 5.** AFM topography images of the two 10-layer compound **1** films at room temperature deposited on bare $SiO_2$/Si substrate (scan range: 5 × 5 $\mu m^2$; height: 0−20 nm; tapping mode) (A), HMDS-treated $SiO_2$/Si substrate (scan range: 5 × 5 $\mu m^2$; height: 0−40 nm; tapping mode) (B), and OTS-treated $SiO_2$/Si substrate (scan range: 5 × 5 $\mu m^2$; height: 0−40 nm; tapping mode) (C).

$[Pc(15C5)_4]Eu[Pc(15C5)_4]Eu[Pc(OC_8H_{17})_8]$, which also assemble with a "face-on" configuration.[28] Inspection of these images reveals that surface treatment with HMDS and OTS on the $SiO_2$/Si substrate induces a significant change in the grain size and density of molecular aggregates due to the morphological change at the surface but not on the aggregate growth mode. The average size of aggregates deposited on the bare $SiO_2$/Si substrate is 97 nm, as shown in Figure 1A, whereas the sizes are 232 and 296 nm on the HMDS-treated $SiO_2$/Si substrate and OTS-treated $SiO_2$/Si substrate, respectively (Figure 1B,C). As can be expected, the increase in the grain size of molecular aggregates led to smaller density of grain boundaries, which act as traps for charge carriers. As a consequence, the increase in the regularity of aggregate shape and size distribution is expected to induce a reduction in the boundaries and carrier traps in the film and result in improved carrier mobility. This is verified by the OFET performance as detailed below.

Interestingly, despite the "edge-on" manner of the molecules on the substrate surface, compound **2** also forms cofacial spherical aggregates (Figure S6 in the Supporting Information). Surface treatment with HMDS on the $SiO_2$/Si substrate also improves the film quality of this compound by reducing the aggregate boundaries and carrier traps in the film. However, the molecular aggregates of triple-decker **2** deposited on the HMDS-$SiO_2$/Si substrates are not as regular as that for compound **1**; their diameter ranges from 127 to 353 nm. The difference in the aggregate morphology of these two compounds can be ascribed to the adhesive effect of different crown ether substituents which provide additional driving force for aggregation and direct the formation of different aggregates in the LB film. As can be expected, despite the *H*-aggregates formed by compound **2**, the inhomogeneous patterns of the molecular packing induce relatively large gaps and cracks between aggregate domains, leading to negative effect on the carrier mobility of corresponding OFET device.[36] The difference in the morphology of these two different triple-decker complexes in solid films reveals the crucial role of crown ether substituents in triple-decker molecules in controlling the molecular packing conformation, which in turn results in different manner in the OFET character of these two complexes.[9]

The OFET devices were fabricated from both triple-decker complexes with top contact configuration. The heavily doped

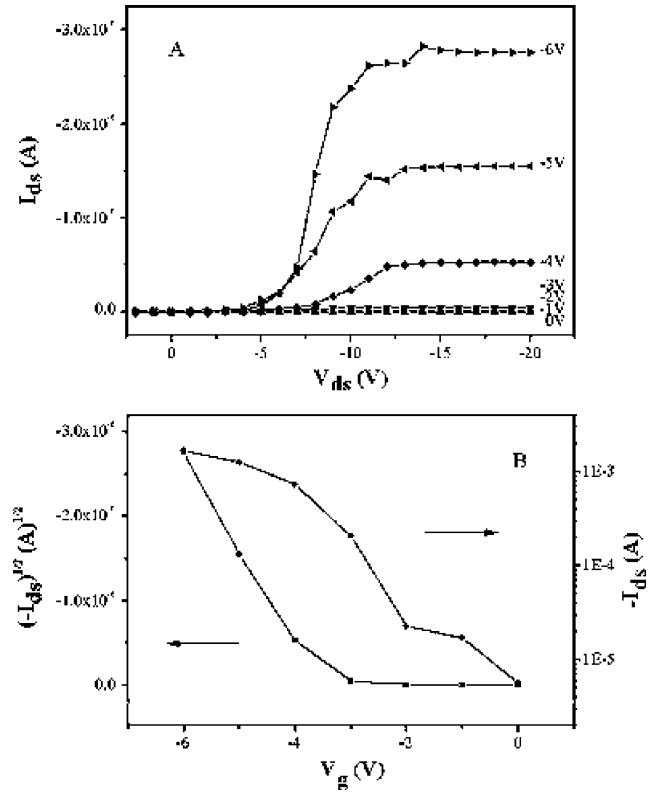


**Figure 6.** Drain-source current ($I_{ds}$) versus drain−source voltage ($V_{ds}$) characteristic at different gate voltage (A) and transfer characteristic at $V_{ds}$ = −20 V (B) for the OFET of compound **1** on the HMDS-treated $SiO_2$/Si substrate.

silicon layer functioning as the gate electrode and the source−drain gold electrodes with the dimension of 28.6-mm width and 0.24-mm length were thermally evaporated onto a 500-nm-thick $SiO_2$ dielectric layer by use of a shadow mask. The semiconductor layer of amphiphilic heteroleptic tris(phthalocyaninato) europium complexes was deposited by LB technique, as shown in Figure 4.[37] The devices were dried in vacuum at room temperature for 10 days before electronic testing, which was carried out at ambient temperature and open to air.

The OFET devices show typical *p*-channel characteristics, as shown in Figures 6 and S7−S10 in the Supporting Information. The carrier mobility ($\mu$) was calculated by using the saturation region transistor equation, $I_{ds} = (W/2L)\mu C_0(V_g$

(36) Xiao, K.; Liu, Y.; Yu, G.; Zhu, D. *Appl. Phys. A* **2003**, *77*, 367–370.

(37) Di, C.; Yu, G.; Liu, Y.; Xu, X.; Wei, D.; Song, Y.; Sun, Y.; Wang, Y.; Zhu, D.; Liu, J.; Liu, X. *J. Am. Chem. Soc.* **2006**, *128*, 16418–16419.

$- V_t)^2$, where $I_{ds}$ is the source−drain current, $V_g$ the gate voltage, $C_0$ the capacitance per unit area of the dielectric layer, and $V_t$ the threshold voltage.[38] Experimental results indicate that, on the bare $SiO_2$/Si substrate, the devices fabricated from triple-decker **1** display relatively poor OFET performance with the carrier mobility for hole of 0.03 $cm^2$ $V^{-1}$ $s^{-1}$ and current modulation of $2.32 \times 10^3$, respectively (Figure S7 in the Supporting Information). Surface treatment with HMDS on the $SiO_2$/Si substrates leads to significant increase in the OFET performance of this compound with the carrier mobility for hole and current modulation amounting 0.31 $cm^2$ $V^{-1}$ $s^{-1}$ and $8.59 \times 10^4$, respectively, as shown in Figure 6. In line with the film morphology investigation result, application of OTS-treated $SiO_2$/Si substrate induces further improvement in the OFET performance of this compound by increasing the current modulation to $7.91 \times 10^5$ with the carrier mobility remained in the same range of 0.33 $cm^2$ $V^{-1}$ $s^{-1}$ (Figure S8 in the Supporting Information). This is also true for the devices fabricated from compound **2**. Without substrate surface treatment, the OFETs of this complex display carrier mobility for hole of 0.02 $cm^2$ $V^{-1}$ $s^{-1}$ and current modulation of $5.5 \times 10^3$, respectively (Figure S9 in the Supporting Information). However, the devices fabricated from triple-decker **2** using HMDS-treated $SiO_2$/Si substrates show carrier mobility in the order of 0.28 $cm^2$ $V^{-1}$ $s^{-1}$, similar to that of compound **1**, as shown in Figure S10 in the Supporting Information, and current modulation of $1.73 \times 10^5$. This result appears strange at first glance as more intense $\pi-\pi$ interaction between neighboring molecules in the face-to-face connected *H*-aggregates than in edge-to-edge connected *J*-aggregates should induce higher carrier mobility, which, however, can be rationalized by the significant better film quality of compound **1** than **2** as detailed above.

## Conclusions

In summary, two new sandwich tris(phthalocyaninato) europium complexes with hydrophilic 12-crown-4 or 18-crwon-6 heads and hydrophobic octyloxy tails have been developed as novel organic semiconductors. The OFET devices fabricated from these heteroleptic tris(phthalocyaninato) europium complexes show good carrier mobility for holes. However, the current flows in a direction parallel to the aromatic phthalocyanine rings in the devices fabricated from triple-decker complex with 12-crown-4 hydrophilic substituents but in a direction along the long axis of the assembly composed of face-to-face aggregated triple-decker molecules with 18-crown-6 groups. Surface treatment with HMDS and OTS on the $SiO_2$/Si substrates is revealed to significantly improve the device performance. The present work, representing a new effort toward knowing the information between molecular structure, film structure, and OFET functional properties, sheds further light on devising molecular materials for OFET devices.

## Experimental Section

**Measurements.** $^1$H NMR spectra were recorded on a Bruker DPX 300 spectrometer (300 MHz) in $CDCl_3$ using the residual solvent resonance of $CHCl_3$ at 7.26 ppm relative to that of $SiMe_4$ as internal reference. Electronic absorption spectra were recorded on a Hitachi U-4100 spectrophotometer. Low angle X-ray diffraction experiment was carried out on a Rigaku D/max-$\gamma$B X-ray diffractometer. Morphology examination was carried out on a Veeco Nanoscope Multimode III SPM with tapping mode. MALDI-TOF mass spectra were taken on a Bruker BIFLEX III ultra-high resolution Fourier transform ion cyclotron resonance mass spectrometer with α-cyano-4-hydroxycinnamic acid as matrix. Elemental analyses were performed by the Institute of Chemistry, Chinese Academy of Sciences. Electrochemical measurements were carried out with a BAS CV-50W voltammetric analyzer. The cell comprised inlets for a glassy carbon disk working electrode of 3.0 mm in diameter and a silver-wire counter electrode. The reference electrode was $Ag/Ag^+$ (0.01 mol $dm^{-3}$), which was connected to the solution by a Luggin capillary whose tip was placed close to the working electrode. It was corrected for junction potentials by being referenced internally to the ferrocenium/ferrocene ($Fc^+$/Fc) couple [$E_{1/2}(Fc^+/Fc) = 0.50$ V vs SCE]. Typically, a 0.1 mol $dm^{-3}$ solution of $[Bu_4N][ClO_4]$ in $CH_2Cl_2$ containing 0.5 mmol $dm^{-3}$ of sample was purged with nitrogen for 10 min, then the voltammograms were recorded at ambient temperature. The scan rate was 20 and 10 mV $s^{-1}$ for CV and DPV, respectively.

**Thin Film Deposition and Characterization.** The solution of $[Pc(mCn)_4]Eu[Pc(mCn)_4]$ ($m = 12$, $n = 4$; $m = 18$, $n = 6$) (**1**, **2**) dissolved in $CH_2Cl_2$ ($1.30 \times 10^{-5}$ to $1.59 \times 10^{-5}$ mol $L^{-1}$) was spread onto ultrapure water (resistivity: 18 MΩ $cm^{-1}$, pH: 6.4) subphase surface. The monolayer properties were studied by measuring pressure−area isotherms on a NIMA System 622 LB trough. All the LB films were deposited onto hydrophobic quartz plates by the vertical dipping method with a dipping speed of 8 mm $min^{-1}$ while the surface pressure was kept at 22 mN $m^{-1}$. Three kinds of quartz plates including the bare $SiO_2$/Si substrate, HMDS-treated $SiO_2$/Si substrate, and OTS-treated $SiO_2$/Si substrate were employed for the LB film deposition.

**OFET Device Fabrication.** The heavily doped silicon layer functioning as the gate electrode and the source−drain electrodes were thermally evaporated onto the LB films by use of a shadow mask. These electrodes have a width (*W*) of 28.6 mm and channel length (*L*) of 0.24 mm. The ratio of the width to the length (*W*/*L*) of the channel was then 119. The oxide layer of 5000 Å is the gate dielectric having a capacitance per unit area of 10 nF $cm^{-2}$. Surface treatment for $SiO_2$/Si substrates was performed according to literature method using HMDS and OTS, respectively, as detailed below.[39] The electric characteristics of these devices were measured under air. The current−voltage characteristics were obtained with a Hewlett-Packard 4140B parameter analyzer at room temperature.

A drop of HMDS was added to the cell culture dish (90 mm), which contained cleaned $SiO_2$/Si substrates. Then the cell culture dish was put into an airtight vial overnight. After being taken out, the substrates were rinsed with chloroform and methanol, respectively, to remove the redundant HMDS. To treat the substrates with OTS, cleaned $SiO_2$/Si substrates were placed in a flask under nitrogen, which contained one drop of OTS. The flask was heated at 120° for 3 h in a vacuum oven. After being cooled to room temperature, the substrates were rinsed with chloroform and

(38) Sze, S. M. *Physics of Semiconductor Devices*; Wiley & Sons: New York, 1981.

(39) Chen, H. Z.; Ling, M. M.; Mo, X.; Shi, M. M.; Wang, M.; Bao, Z. *Chem. Mater.* **2007**, *19*, 816–824.

methanol, then ultrasonically cleaned with hexane for 15 min to remove the residual organic contamination, and then dried with nitrogen.

**Chemicals.** Anhydrous TCB, HMDS, and OTS were purchased from Aldrich. Dichloromethane for voltammetric studies was freshly distilled from $CaH_2$ under nitrogen. Column chromatography was carried out on silica gel (Merck, Kieselgel 60, 70−230 mesh) with the indicated eluents. All other reagents and solvents were used as received. The compounds 4,5-dibromobenzo-(18-crown-6),[20,21] $Eu(acac)_3 \cdot H_2O$,[40] $H_2[Pc(OC_8H_{17})_8]$,[23] and $Eu[Pc(mCn)_4]_2$ ($m = 12$, $n = 4$; $m = 18$, $n = 6$) were prepared according to the published procedures.

**Preparation of 1,2-Bis(2-chloroethoxy)ethane.** The mixture of triethyleneglycol (37 mL, 0.28 mol) and pyridine (49 mL, 0.61 mol) in benzene (250 mL) was heated to reflux, and then thionyl chloride (44.2 mL, 0.61 mol) was added dropwise over 3 h. The mixture was kept on refluxing for another 16 h and then cooled to room temperature. Then hydrochloric acid (6.3 mL, 11.8 M) diluted with water (50 mL) was added dropwise in 15 min. The upper benzene solution was separated, and after evaporation under reduced pressure, the target compound 1,2-bis(2-chloroethoxy)ethane was obtained as a lucid oil (47.1 g, 90%). $^1$H NMR ($CDCl_3$, 300 MHz): $\delta$ 3.44−3.46 (m, 4 H, Cl−$CH_2$), 3.37−3.38 (m, 8 H, $CH_2$−O−$CH_2$). MS ($EI^+$): $M^+ - 80$ (107), (−$OCH_2CH_2Cl$); $M^+ - 94$ (94), (−$CH_2OCH_2CH_2Cl$); $M^+ - 107$ (80), (−$CH_2CH_2OCH_2CH_2Cl$); $M^+ - 123$ (64), (−$OCH_2CH_2OCH_2CH_2Cl$). Anal. Calcd for $C_6H_{12}O_2Cl_2$: C, 38.52; H, 6.47. Found: C, 37.95; H, 6.80.

**Preparation of Benzo-12-crown-4.** Sodium hydroxide (12 g, 0.30 mol) and lithium hydroxide (12 g, 0.50 mol) dissolved in water (50 mL) were mixed with the *n*-butanol (740 mL) solution containing catechol (30 g, 0.27 mol) under a slow stream of argon gas. The mixture was then heated to reflux for half an hour, and the liquid 1,2-bis(2-chloroethoxy)ethane was added dropwise in 20 min. After being refluxed for another 26 h, the reaction mixture was cooled to room temperature and hydrochloric acid (9 mL) was added. After being kept overnight, the mixture was filtrated, and the filtrate, after removing solvent under reduced pressure, was redissolved in chloroform and washed with water (100 mL × 3). The organic layer was collected, and the solvent was removed under reduced pressure. The yellow oil obtained was then applied on an $Al_2O_3$ column (acid, 200−300 mesh) with *n*-heptane/ethyl acetate (5:1) as eluent. Repeated chromatography followed by being poured into ice water gave pure target product as white powder (25.4 g, 45%). $^1$H NMR ($CDCl_3$, 300 MHz): 6.94−7.00 (m, 4 H, benzene ring), 4.17−4.19 (m, 4 H, crown ether), 3.85−3.87 (m, 4 H, crown ether), 3.80 (s, 4 H, crown ether). MS ($EI^+$): $M^+$ (225); $M^+ - 44$ (181), (−$CH_2CH_2O$−); $M^+ - 60$ (165), (−$OCH_2CH_2O$−); $M^+ - 88$ (137), (−$CH_2OCH_2CH_2OCH_2$−); $M^+ - 116$ (109), (−$CH_2CH_2OCH_2CH_2OCH_2CH_2$−). Anal. Calcd for $C_{12}H_{16}O_4$: C, 64.27; H, 7.19. Found: C, 64.58; H, 7.05.

**Preparation of 4,5-Dibromobenzo-12-crown-4.** To the solution of benzo-12-crown-4 (4.5 g, 0.02 mol) dissolved in acetic acid (18 mL), a solution of bromine (2.1 mL, 0.04 mol) in acetic acid (10 mL) was added dropwise over 4 h, and the mixture was stirred for another 30 h under room temperature. The mixture was filtrated and washed with boiled petroleum ether. The residue was chromatographed on a silica gel column with *n*-heptane/ethyl acetate (1:1) as eluent. Repeated chromatography followed by recrystallization in *n*-hexane gave pure target compound as white powder (6.0 g, 78%). $^1$H NMR ($CDCl_3$, 300 MHz): 7.21 (s, 2 H, benzene ring), 4.14−4.17 (m, 4 H, crown ether), 3.83−3.85 (m, 4 H, crown ether), 3.76 (s, 4 H, crown ether). MS ($EI^+$): $M^+$ (382); $M^+ - 28$ (354), (−$CH_2CH_2$−); $M^+ - 60$ (322), (−$OCH_2CH_2O$−); $M^+ - 88$ (294), (−$CH_2OCH_2CH_2OCH_2$−); $M^+ - 116$ (266), (−$CH_2CH_2OCH_2CH_2OCH_2CH_2$−); $M^+ - 148$ (234), (−$OCH_2CH_2OCH_2CH_2OCH_2CH_2O$−); $M^+ - 308$ (74), (−$OCH_2CH_2OCH_2CH_2OCH_2CH_2O$−, −Br−, −Br−). Anal. Calcd for $C_{12}H_{14}O_4Br_2$: C, 37.73; H, 3.69. Found: C, 38.12; H, 3.36.

**Preparation of 4,5-Dicyanobenzo-12-crown-4.** A mixture of 4,5-dibromobenzo-12-crown-4 (2.1 g, 5.55 mmol), CuCN (1.8 g, 20.43 mmol), and pyridine (0.5 mL) in DMF (35 mL) was heated to reflux for 20 h under a slow stream of argon gas. After being cooled to room temperature, the mixture was poured to ammonia (135 mL) and blown with fresh air. Then the solution was extracted with chloroform (100 mL × 3). The combined extracts were washed with water, dried over anhydrous $MgSO_4$, and evaporated. The crude product was chromatographed over a silica gel column with petroleum ether/ethyl acetate (5:1) as eluent. The solvent was evaporated under reduced pressure, giving white target compound 4,5-di(12-crown-4)phthalonitrile (0.9 g, 69%). $^1$H NMR ($CDCl_3$, 300 MHz): 7.29 (s, 2 H, benzene ring), 4.26−4.17 (m, 4 H, crown ether), 3.83−3.85 (m, 4 H, crown ether), 3.76 (s, 4 H, crown ether). MS ($EI^+$): $M^+$ (274); $M^+ - 28$ (246), (−$CH_2CH_2$−); $M^+ - 60$ (214), (−$OCH_2CH_2O$−); $M^+ - 88$ (186), (−$CH_2OCH_2CH_2OCH_2$−); $M^+ - 116$ (158), (−$CH_2CH_2OCH_2CH_2OCH_2CH_2$−); $M^+ - 148$ (126), (−$OCH_2CH_2OCH_2CH_2OCH_2CH_2O$−); $M^+ - 200$ (74), (−$OCH_2CH_2OCH_2CH_2OCH_2CH_2O$−, −CN−, −CN−). Anal. Calcd for $C_{14}H_{14}O_4N_2$: C, 61.31; H, 5.15; N, 10.21. Found: C, 61.58; H, 5.36; N, 10.48.

**Preparation of $Eu[Pc(12C4)_4]_2$.** A mixture of 4,5-dicyanobenzo-12-crown-4 (185 mg, 0.68 mmol) and $Eu(acac)_3 \cdot H_2O$ (41 mg, 0.09 mmol) in *n*-pentanol (6 mL) was heated to reflux under nitrogen for 24 h. After being cooled to room temperature, the mixture was evaporated under reduced pressure, and the residue was chromatographed on a silica gel column with $CHCl_3$ as eluent. A green band containing the target double-decker complex was developed. Repeated chromatography followed by recrystallization from $CHCl_3$ and *n*-hexane gave pure target compound as a dark powder (60 mg, 30%). $^1$H NMR ($CDCl_3$, 300 MHz): $\delta$ 10.97 (s, 16 H, Pc ring), 6.00 (s, 16 H, crown ether), 5.55 (m, 16 H, crown ether), 4.96 (s, 16 H, crown ether), 4.66 (m, 16 H, crown ether), 4.32−4.49 (m, 32 H, crown ether). MALDI-TOF MS: an isotopic cluster peaking at $m/z$ 2346.0, calcd for $C_{112}H_{112}N_{16}O_{32}Eu$, $[M]^+$ 2346.1. Anal. Calcd for $C_{112}H_{112}EuN_{16}O_{32}$: C, 57.34; H, 4.81; N, 9.55. Found: C, 57.52; H, 4.71; N, 9.32.

**Preparation of $Eu[Pc(18C6)_4]_2$.** A mixture of 4,5-dicyanobenzo-18-crown-6 (427 mg, 1.20 mmol) and $Eu(acac)_3 \cdot H_2O$ (95 mg, 0.21 mmol) in *n*-pentanol (6 mL) was heated to reflux under nitrogen for 24 h. After being cooled to room temperature, the mixture was evaporated under reduced pressure, and the residue was chromatographed on a silica gel column with $CHCl_3$ as eluent. A green band containing the target double-decker complex was developed. Repeated chromatography followed by recrystallization from $CHCl_3$ and *n*-hexane gave pure target compound as a dark powder (37 mg, 31%). $^1$H NMR ($CDCl_3$, 300 MHz): $\delta$ 10.65 (s, 16 H, Pc ring), 6.06 (s, 16 H, crown ether), 5.45 (m, 16 H, crown ether), 4.35−4.77 (m, 32 H, crown ether), 3.71−4.32 (m, 96 H, crown ether). MALDI-TOF MS: an isotopic cluster peaking at $m/z$ 3050.8, calcd for $C_{144}H_{176}N_{16}O_{48}Eu$, 3051.0. Anal. Calcd for $C_{144}H_{176}EuN_{16}O_{48}$: C, 56.69; H, 5.81; N, 7.35. Found: C, 56.74; H, 5.62; N, 7.21.

**General Procedure for the Preparation of $[Pc(mCn)_4]Eu[Pc(mCn)_4]Eu[Pc(OC_8H_{17})_8]$ ($m = 12$, $n = 4$; $m = 18$, $n = 6$) (1, 2).** A mixture of $Eu(acac)_3 \cdot H_2O$ (27 mg, 0.058 mmol), $Eu[Pc(mCn)_4]_2$ (0.02 mmol), and excess amount of $H_2Pc(OC_8H_{17})_8$ (0.03 mmol) in TCB (6 mL) was refluxed for about 4 h under a slow stream of nitrogen. The resulting blue solution was cooled to room temperature, and then the volatiles were removed under

(40) Sitites, J. G.; McCarty, C. N.; Quill, L. L. *J. Am. Chem. Soc.* **1948**, *70*, 3142–3143.

reduced pressure. The residue was chromatographed on a silica gel column. A small amount of unreacted $H_2Pc(OC_8H_{17})_8$ was eluted out first with $CHCl_3$ as eluent. Then the column was eluted with $CHCl_3$/MeOH (97:3), and a blue band containing the target triple-decker compound was developed. The latter fraction was collected and chromatographed again using toluene/MeOH (98:2) as eluent. Repeated chromatography followed by recrystallization from a mixture of $CHCl_3$ and MeOH gave pure target triple-decker samples as a dark powder in relatively good yield.

**$[Pc(12C4)_4]Eu[Pc(12C4)_4]Eu[Pc(OC_8H_{17})_8]$ (1):** (24.2 mg, 30%). $^1$H NMR ($CDCl_3$, 300 MHz): 12.52 (br s, 8 H, Pc ring), 9.67 (s, 8H, Pc ring), 9.29 (br s, 8H, Pc ring), 6.92−7.01 (m, 16H, $CH_2$ of crown ether), 5.74−5.78 (m, 16H, $CH_2$ of crown ether), 5.65−5.69 (m, 16H, $CH_2$ of octyloxy), 5.03−5.11 (m, 16H, $CH_2$ of octyloxy), 4.92−4.96 (m, 16H, $CH_2$ of crown ether), 4.70−4.76 (m, 16H, $CH_2$ of crown ether), 4.38−4.51 (m, 16H, $CH_2$ of crown ether), 4.03−4.07 (m, 16H, $CH_2$ of crown ether), 2.66−2.81 (m, 16H, $CH_3$ of octyloxy), 2.24−2.34 (m, 16H, $CH_2$ of octyloxy), 1.58−1.94 (m, 16H, $CH_3$ of octyloxy), 1.08−1.13 (m, 16H, $CH_2$ of octyloxy). MALDI-TOF MS: an isotopic cluster peaking at *m*/*z* 4036.4, calcd for $(M)^+$, 4036.3. Anal. Calcd for $C_{208}H_{256}Eu_2N_{24}O_{40}$: C, 61.89; H, 6.39; N, 8.33. Found: C, 61.32; H, 6.31; N, 8.32.

**$[Pc(18C6)_4]Eu[Pc(18C6)_4]Eu[Pc(OC_8H_{17})_8]$ (2):** (19.0 mg, 20%). $^1$H NMR ($CDCl_3$, 300 MHz): 12.22 (s, 8 H, Pc ring), 9.20 (br s, 16H, Pc ring), 6.61 (br s, 16H, $CH_2$ of crown ether), 5.59−5.67 (m, 16H, $CH_2$ of crown ether), 5.59−5.67 (m, 16H, $CH_2$ of octyloxy), 4.94 (br s, 16H, $CH_2$ of crown ether), 4.67−4.74 (m, 32H, $CH_2$ of crown ether),4.67−4.74 (m, 16H, $CH_2$ of octyloxy), 4.51 (br s, 48H, $CH_2$ of crown ether), 4.01−4.08 (m, 16H, $CH_2$ of crown ether), 3.74−3.83 (m, 16H, $CH_2$ of crown ether), 2.50−2.61 (m, 16H, $CH_2$ of octyloxy), 2.08−2.10 (m, 16H, $CH_3$ of octyloxy), 1.25−1.98 (m, 48H, $CH_2$ of octyloxy), 0.86−1.01 (m, 24H, $CH_3$ of octyloxy). MALDI-TOF MS: an isotopic cluster peaking at *m*/*z* 4741.4, calcd for $(M)^+$, 4141.2. Anal. Calcd for $C_{240}H_{320}Eu_2N_{24}O_{56}$: C, 60.80; H, 6.80; N, 7.09. Found: C, 60.28; H, 6.75; N, 7.09.

**Acknowledgment.** Financial support from the Natural Science Foundation of China, Ministry of Education of China, and Shandong University is gratefully acknowledged.

**Supporting Information Available:** Additional spectral and experimental data including the isotopic pattern for the molecular ion of **1**, $^1$H NMR spectrum of compound **1** in $CDCl_3$, $^1$H-$^1$H COSY spectrum of compound **1** $CDCl_3$, dipper area-time isotherm for compounds **1** and **2**, low angle X-ray diffraction patterns of the LB films of compounds **2**, AFM topography images of the two 10-layer compound **2** film, current-voltage characteristics of compounds **1** and **2** on different substrates, and electronic absorption spectral data for the triple-deckers **1** and **2**. This material is available free of charge via the Internet at http://pubs.acs.org.

IC801040Z